Comparison of the magnetic properties and the spin dynamics in heterometallic antiferromagnetic molecular rings

H. Amiri,[1,2,*] A. Lascialfari,[1,2,3] Y. Furukawa,[4] F. Borsa,[2,4] G. A. Timco,[5] and R. E. P. Winpenny[5,6]

[1]*Department of Molecular Sciences Applied to Biosystems, Università degli Studi di Milano, I-20134 Milan, Italy*
[2]*Department of Physics "A. Volta" and CNISM, Università di Pavia, I-27100 Pavia, Italy*
[3]*Centro S3, CNR-Istituto di Nanoscienze, I-41125 Modena, Italy*
[4]*Ames Laboratory and Department of Physics and Astronomy, Iowa State University, Ames, Iowa 50011, USA*
[5]*The Lewis Magnetism Laboratory, School of Chemistry, The University of Manchester, Oxford Road,*
Manchester M13 9PL, United Kingdom
[6]*The Photon Science Institute, The University of Manchester, Oxford Road, Manchester M13 9PL, United Kingdom*
(Received 19 July 2010; published 12 October 2010)

We present a comparison of the results obtained in the antiferromagnetic (AFM) homometallic ring Cr_8 with the results in three heterometallic rings with a Cr ion replaced by Cd, Ni, and Fe ions, i.e., Cr_7Cd, Cr_7Ni, and Cr_7Fe, respectively. The experimental results include magnetic susceptibility, ^{1}H nuclear-magnetic-resonance (NMR) spectra, spin-spin and spin-lattice relaxation rates data, collected in the temperature range $1.65 < T < 300$ K at two applied magnetic fields. The data include both new results and previously published data. The static magnetic properties derived from susceptibility and ^{1}H NMR linewidth can be analyzed in a simple way in terms of the properties of the individual ions constituting the ring and their nearest-neighbor antiferromagnetic exchange coupling. The nuclear-spin-lattice relaxation rate at low temperature can be described phenomenologically by a model, which assumes a single-correlation time for the relaxation of the magnetization, as used previously for homometallic AFM rings. The correlation frequencies obtained from the fit of the data, increase by as much as two orders of magnitude in the Cr_7Ni and Cr_7Fe rings with respect to the homometallic ring Cr_8 and the diamagnetically substituted Cr_7Cd ring. This result can be explained qualitatively in terms of a change in spin-phonon coupling due to the enhancement of crystal-field effects in the heterometallic rings. For a more quantitative analysis one should take into account the multi-Lorentzian behavior of the spin-spin correlation function for which detailed theoretical calculations are required. At temperatures higher than the magnetic exchange energy J/k_B, the mechanism for nuclear-spin-lattice relaxation changes since the fluctuations of the moments of the magnetic ions become weakly correlated. We find a fluctuation frequency much higher in the heterometallic rings as a result of the perturbation introduced by the substituted magnetic ion.

PACS number(s): 75.50.Xx, 75.75.Fk, 76.60.Es

I. INTRODUCTION

Molecular nanomagnets have opened the possibility to investigate new interesting phenomena in magnetism.[1–3] In molecular nanomagnets, investigation of the magnetic properties and of the spin dynamics of a single molecule is possible because the magnetic cores of the individual molecules are isolated from each other by a shell of bulky organic ligands so that the intermolecular magnetic interactions (usually dipolar) are very weak compared to the intramolecular exchange interactions.[3]

A specific type of nanomagnets are the antiferromagnetic (AFM) molecular rings, i.e., magnetic molecules with an even number of uniformly spaced paramagnetic metal ions arranged as a planar ring and interacting via strong nearest-neighbor antiferromagnetic exchange interactions. If the ring contains just one type of magnetic ion, then it is called homometallic (e.g., Cr_8 which is characterized by a singlet zero-field ground state with total spin $S_T=0$).[4] On the other hand by substituting one of the paramagnetic ions with a nonmagnetic ion (e.g., Cd) or with an ion with different magnetic moment (e.g., Fe^{2+} and Ni^{2+}) one obtains a heterometallic AFM ring with a magnetic ground state $S_T \neq 0$ and with different static and dynamical magnetic properties.[5] Of particular interest are the effects of redistribution of the local

magnetic moment density in the heterometallic rings[6] and the changes in the spin dynamics. Since the ground state of these heterometallic AFM rings could be used for implementation of qubits for quantum computation, and the synthesis of heterometallic rings containing coupled molecules could lead to quantum entanglement,[7,8] the investigation of the magnetic properties and particularly of the spin dynamics which can affect the quantum coherence or decoherence in these heterometallic rings is of great relevance.

Nuclear magnetic resonance (NMR) has been proved to be an efficient local probe of both static and dynamic properties of magnetic molecules[9] and used in combination with thermodynamic magnetization measurements can give a good characterization of the magnetic properties and the spin dynamics in the heterometallic rings. In this paper we will compare the results in the homometallic AFM ring Cr_8 with the results in three heterometallic rings with a Cr ion replaced by Cd, Ni, and Fe ions, i.e., Cr_7Cd, Cr_7Ni, and Cr_7Fe, respectively. In the ground state, these rings are characterized by a total spin $S_T=0$, 1/2, 1/2, and 3/2, for the Cr_8, Cr_7Fe, Cr_7Ni, and Cr_7Cd, respectively, resulting from AFM interactions J between nearest-neighbor Cr^{3+} ($s=3/2$) ions and J' between Cr^{3+} and the substituted ions: Fe^{2+} ($s=2$), Ni^{2+} ($s=1$), and Cd^{2+} ($s=0$). The paper is organized as follows. In Sec. II we summarize briefly the synthesis of the compounds
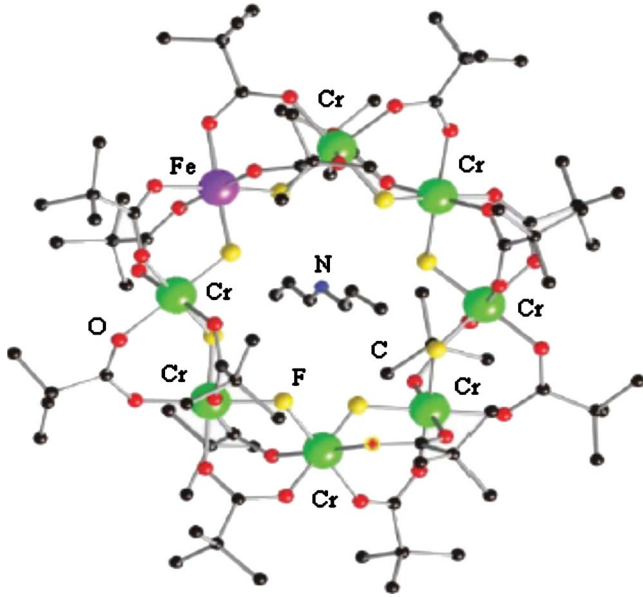
$$\chi = \lim_{H \to 0} M/H,$$

which for paramagnets far from saturation can be approximated by M/H, have been performed with a superconducting quantum interference device (SQUID) magnetometer on different rings, at two different external magnetic fields. The data for Cr_8 were taken in polycrystalline powder sample while in the other three rings the data were taken on single crystals with H oriented perpendicular to the molecular c axis which is perpendicular to the plane formed by the magnetic ions, i.e., to the plane of the ring. In the temperature and field interval measured here the susceptibility is found to be isotropic, within the experimental error.

For a straightforward comparison of the results in the four rings, we show in Fig. 2 the susceptibility times temperature vs temperature, which corresponds to the plot of the effective Curie constant as a function of temperature. The data for Cr_7Fe are from a previous publication.[13] All other data are new although partial susceptibility data have been published earlier for Cr_7Ni (Ref. 14) and Cr_8 (Refs. 9, 15, and 16).

The upper dashed lines in Fig. 2 correspond to the value of the Curie constant $C = Ng^2\mu_B^2[s(s+1)]/3k_B$, where it was assumed for the g factor $g=2$ for both Cr^{3+} and the substituted ions while the spin s for Cr^{3+} is 3/2 and for the Fe^{2+}, Ni^{2+}, and Cd is 2, 1, and 0, respectively. The experimental data in Fig. 2 lie below the high-T limit as expected in presence of AFM coupling but seem to bend toward the limit calculated for noninteracting ions with the given spin s value and negligible single ion anisotropy ($g=2$). The low-temperature dashed-dotted lines represent the Curie constant for a single total spin, $S_T = 0, 1/2, 1/2$, and 3/2, for the Cr_8, Cr_7Fe, Cr_7Ni, and Cr_7Cd, respectively, with $g=2$. The agreement is good indicating that at low temperature the rings occupy a collective ground state characterized by a total spin value as given above. The calculated Curie constants for both high- and low-temperature limits are summarized in Table I.

For temperatures above 100 K the magnetic ions are weakly correlated and their susceptibility can be described, in the molecular-field approximation, in terms of the nearest-neighbor Cr^{3+}-Cr^{3+} interaction J and the interaction J' between Cr^{3+} ions and the substituted ion.

In Fig. 3 we have plotted the inverse susceptibility vs temperature for the four rings. The high-temperature (above 100 K) results can be fitted reasonably well by using a Curie-Weiss law for the susceptibility, i.e., $1/\chi = [T-\Theta]/C$, with C values calculated above for the high-T limit (see Table I) and by choosing Θ as the only fitting parameter. The Θ values obtained from the fits for different rings are listed in Table I. Assuming that the dominant contribution to the Curie-Weiss temperature Θ comes from the more abundant Cr^{3+} ions and using the molecular-field approximation expression $\Theta = [2zs(s+1)J]/3k_B$, with the number of nearest neighbors of a given moment being $z=2$, we have obtained the AFM coupling constants Cr_7Cd for all the rings.

The exchange constants derived above correspond to a Hamiltonian for the Heisenberg model written as $\sum_{i>j} -2J_{ij}\vec{S}_i \cdot \vec{S}_j$. Since the values of J given in the molecular nanomagnets are normally referred to a Hamiltonian written as

FIG. 1. (Color online) Structure of $(C_4H_9)_2NH_2Cr_7Fe^{2+}F_8(O_2CCMe_3)_{16}$ molecular nanomagnet, in brief Cr_7Fe.

and their crystal structure. In Sec. III the experimental results and data analysis for the magnetization will be presented. In Sec. IV we present in separate sections the static and the dynamic NMR results with their analysis. Sec. V contains a summary of the results and the conclusions.

II. SYNTHESIS AND STRUCTURE

The homometallic ring Cr_8, $[Cr_8F_8(O_2CCMe_3)_{16}]$, has been widely studied,[10,11] both because of its magnetic properties[11] and because it can act as a host for heterometallic substitution.[12] In order to prepare a heterometallic ring one of the chromium ions should be substituted with a metallic ion. In our case the Cr ion is replaced with Cd, Ni, and Fe. Using the same amine as a template for Cr_7M (M=Cd, Ni, and Fe) rings will give us the isostructural Cr_7Cd, Cr_7Ni, and Cr_7Fe rings with the same bond length within the ring. Although the lattices parameters may vary slightly, the structure will be the same. The nearest-neighbor exchange interaction between Cr ions is almost independent from the substituting ion while the exchange interaction between the Cr ion and the substituting ion depends on the type of heterometallic substitution as will be discussed further on. The synthesis procedure for all of them has been reported in Ref. 5.

The schematic structure of a heterometallic ring, for the case that one Cr is replaced with a Fe ion, is shown in Fig. 1. The position of protons in the molecule is important for our ^1H NMR study. Around each Cr there are three closest CH_3 groups. For each CH_3 there are three Cr-H distances: (i) shortest, in the range 4.07–4.32 Å, (ii) middle, in the range 4.48–4.93 Å, and (iii) longest, in the range of 5.47–5.57 Å. Other protons are located even further away from Cr ions.

III. MAGNETIC SUSCEPTIBILITY
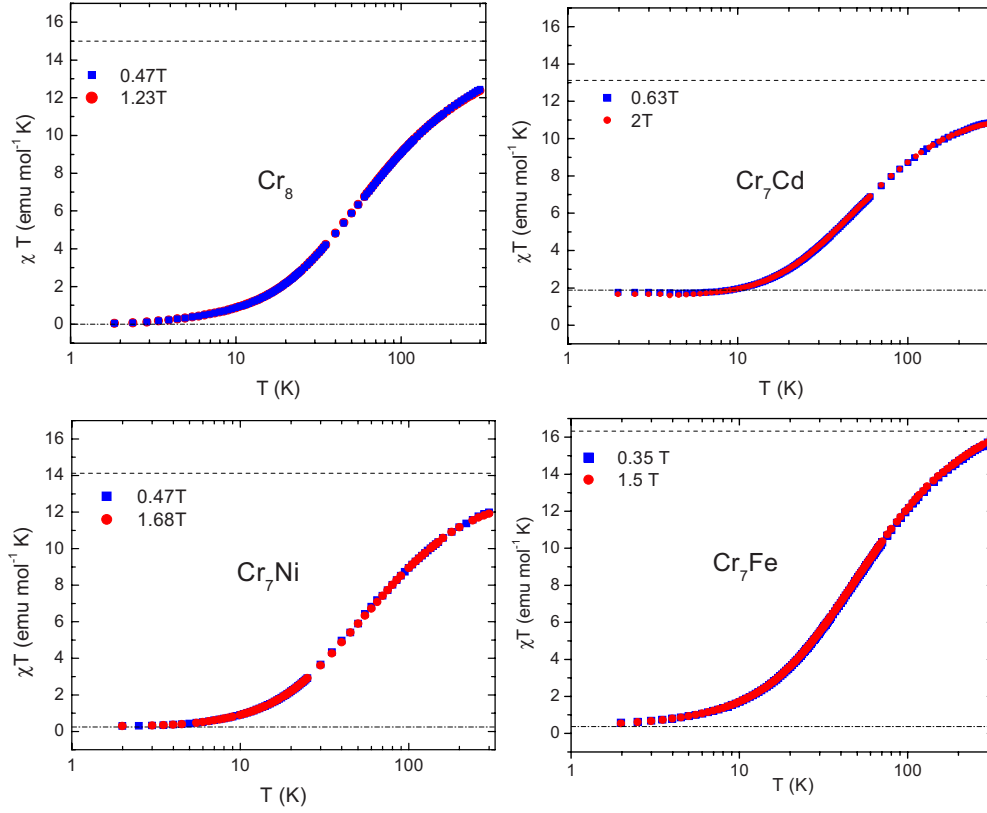
Measurements of magnetic susceptibility

FIG. 2. (Color online) The susceptibility times temperature plotted vs temperature in different magnetic rings at two external magnetic fields. The dashed and dashed-dotted lines are the limiting behaviors at high and low temperatures, respectively, expected for a simple paramagnetic model of the AFM rings (see text).

$\Sigma_{i>j}J_{ij}\vec{S}_i\cdot\vec{S}_j$, we multiply our value by two and change sign in order to compare it with the J constants given in the literatures for AFM rings. The values obtained for J are reported in Table I. The values of J are very similar for all rings except Cr$_7$Fe for which the value is smaller, i.e., $J=13\pm1$ K, indicating a stronger magnetic perturbation of the exchange couplings in the ring as also evident in the dynamic properties discussed in the following section.

The oversimplified analysis presented above is justified by the desire to have a quick comparison of the magnetic properties of the four rings and is in reasonable agreement with more rigorous fits of the susceptibility and analysis of the coupling constants published for some of the rings.[17]

TABLE I. High- and low-temperature limits $C_{\text{high-}T\text{ limit}}$ and $C_{\text{low-}T\text{ limit}}$, respectively, the Curie-Weiss temperature Θ, and the AFM coupling constants for all the investigated rings.

Molecule	$C_{\text{high-}T\text{ limit}}$	$C_{\text{low-}T\text{ limit}}$	Θ (K)	J/k_B (K)
Cr$_8$	15.005	0	−64	25.6
Cr$_7$Cd	13.13	1.875	−58	23.2
Cr$_7$Ni	14.13	0.249	−55	22
Cr$_7$Fe	16.32	0.374	−32	13

IV. NMR EXPERIMENTAL RESULTS AND ANALYSIS

Proton NMR measurements including nuclear-spin-lattice relaxation time (T_1) and spin-spin relaxation time (T_2) were performed using a standard TecMag Fourier-transform pulse NMR spectrometer with short $\pi/2$-$\pi/2$ radio frequency (rf) pulses (1.9–2.2 μs) in the temperature range $1.65 < T < 300$ K. In order to study the temperature dependence of the relaxation times, we used two different cryostats: (a) a continuous flow cryostat in the temperature range $4.2 < T < 300$ K and (b) a bath cryostat in the temperature range $1.65 < T < 4.2$ K. Fourier transform (FT) of half of the echo spin signal yields the NMR spectrum in the case where the whole line could be irradiated with one rf pulse.

The nuclear-spin-lattice relaxation rate T_1^{-1} was determined by monitoring the recovery of the longitudinal nuclear magnetization measured by the spin-echo amplitude obtained with $\pi/2$-$\pi/2$ pulse sequence, following a saturating comb of rf pulses. The length of the rf saturation comb was chosen to insure the best initial saturation conditions which vary depending on temperature and resonance frequency. The recovery of the nuclear magnetization was found to follow a multiexponential law. The effective relaxation rate was determined as described further on.

To perform the spin-spin relaxation time experiments, a standard solid echo ($\pi/2$-$\pi/2$) pulse sequence was used. For all temperatures a single exponential decay of the transverse
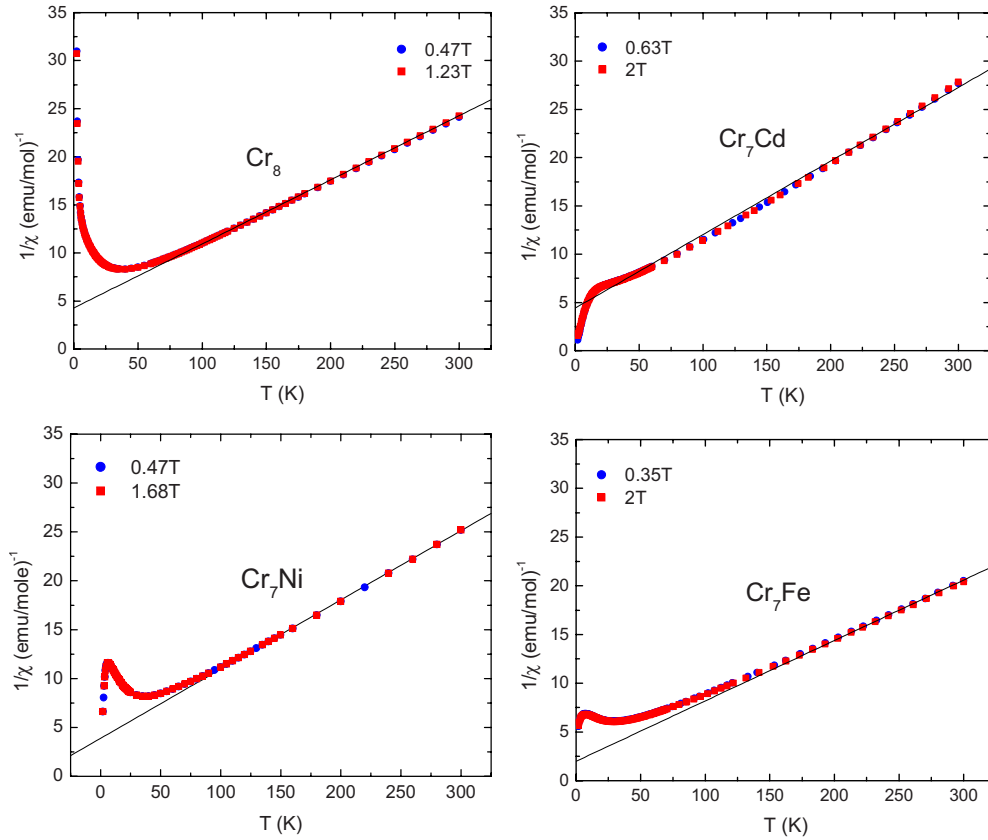
FIG. 3. (Color online) Inverse susceptibility vs temperature in different rings at two external magnetic fields; the solid lines are fits according to the Curie-Weiss law (see text).

nuclear magnetization was observed so that a well-defined spin-spin relaxation time parameter T_2 can be defined.

A. Proton NMR spectra

The proton NMR linewidth full width at half maximum (FWHM) or $\Delta\nu$ for all the rings is shown in Fig. 4 as a function of temperature at two values of the external magnetic field. The magnitude and the temperature dependence of the linewidth are similar in all the rings reflecting the fact that the broadening has the same origin in all of them. In fact the shape and width of the proton NMR spectrum is determined by two main interactions: (i) the nuclear-nuclear dipolar interaction and (ii) the hyperfine interaction of the proton with the neighboring magnetic ions. The first interaction generates a temperature- and field-independent broadening which depends on the hydrogen distribution in the molecule and is thus the same in all molecular magnets independently of their magnetic properties.[9]

The hyperfine field resulting from the interaction of protons with local magnetic moments of Cr^{3+} (Fe^{2+} and Ni^{2+}) may contain contributions from both the classical dipolar interaction and from a direct contact term due to the hybridization of proton s-wave function with the d-wave function of magnetic ions. The dipolar contribution has tensorial character and is thus responsible for the inhomogeneous width of the line due to the random distribution of orientations in a powder sample of the vector joining the nucleus to the elec-

tronic moment and to the many nonequivalent proton sites in the single crystal. The contact interaction, on the other hand, has scalar form and it can generate a shift of the line for certain groups, each one constituted by equivalent protons in the molecule. Since we have not observed any measurable shift of the proton NMR line from the Larmor frequency, we can conclude that the dominant hyperfine interaction is of dipolar origin.

In the usual simple Gaussian approximation for the NMR line shape, the linewidth is proportional to the square root of the second moment, which in turn is given by the sum of the second moments due to the two interactions described above,[18]

$$\text{FWHM} \propto \sqrt{\langle \Delta\nu^2 \rangle_d + \langle \Delta\nu^2 \rangle_m}, \tag{1}$$

where $\langle \Delta\nu^2 \rangle_d$ is the intrinsic second moment due to nuclear-nuclear dipolar interactions and $\langle \Delta\nu^2 \rangle_m$ is the second moment of the local frequency-shift distribution (due to the nearby electronic moments) at the different proton sites of all molecules. The proportionality constant in Eq. (1) is on the order of one depending on the exact shape of the spectrum. We will assume it to be one, for simplicity. The relation between $\langle \Delta\nu^2 \rangle_m$ and the local Cr^{3+}, Fe^{2+}, and Ni^{2+} electronic moments for a simple dipolar interaction is given by[9,18]
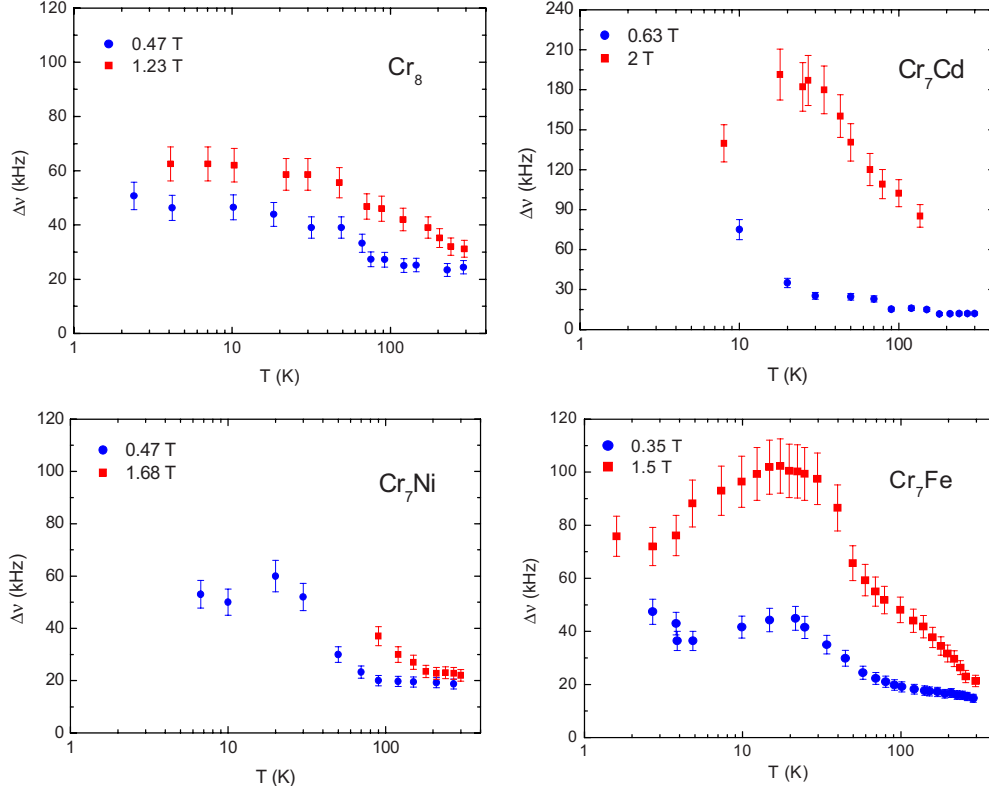
FIG. 4. (Color online) Proton linewidth vs temperature in all the molecular rings at two different external magnetic fields.

$$\langle \Delta \nu^2 \rangle_m = \frac{1}{N} \sum_R \left(\sum_{i \in R} \langle \nu_{R,i} - \nu_L \rangle_{\Delta t} \right)^2$$
$$= \frac{\gamma^2}{N} \sum_R \left[\sum_{i \in R} \sum_{j \in R} \frac{A(\vartheta_{i,j})}{r_{i,j}^3} \langle m_{z,j} \rangle_{\Delta t} \right]^2, \quad (2)$$

where R labels different molecules, i and j span different protons and Cr^{3+} ions within each molecule, N is the total number of probed protons. In Eq. (2), $\nu_{R,i}$ is the NMR resonance frequency of nucleus i and $\nu_L = (\gamma/2\pi)H = \bar{\gamma}H$ is the bare Larmor resonance frequency. The difference between the two resonance frequencies represents the shift for nucleus i due to the local field generated by the nearby moments j. The angular-dependent dipolar coupling constant between nucleus i and electronic moment j is $A(\vartheta_{i,j})$ and $r_{i,j}$ is the corresponding distance. $\langle m_{z,j} \rangle$ is the component of the Cr (Fe and Ni) moment j in the direction of the applied field, averaged over the NMR data acquisition time. In a simple paramagnet one expects $\langle m_{z,j} \rangle = (\chi/N_A)H$ with χ the SQUID susceptibility in electromagnetic unit/mole, N_A Avogadro's number, and H the applied field.[19] We can thus write

$$\langle \Delta \nu^2 \rangle_m = A'_z (\chi H)^2 = A'_z \left(\chi \frac{\nu_L}{\gamma} \right)^2 = A_z \left(\chi \frac{\nu_L}{N_A} \right)^2, \quad (3)$$

where A_z and A'_z are the square dipolar coupling constants averaged over all protons and all orientations expressed in different units.

The experimental results for the magnetic contribution to the linewidth are plotted as a function of the magnetic susceptibility in Fig. 5 for all the molecular rings. As one can see the linear relation, predicted by Eqs. (1) and (3), is well verified. In the fit of Fig. 5 we have neglected the nuclear dipolar contribution in Eq. (1) since at such fields the inhomogeneous contribution to the width is already dominant. The values obtained from the fit are summarized in Table II.

The average square dipolar coupling constants (see Table II) are practically the same in all the rings as expected in view of the same crystal structure and thus the same proton-ion distance. The smaller values for the Ni and Fe substituted rings are probably due to slightly larger distances not revealed by x-ray analysis.

B. NMR signal intensity: Wipe-out effect

The wipe-out effect consists in a progressive loss of measurable NMR signal intensity normally observed in magnetic systems as the temperature is lowered. There is a general consensus that the effect has to be ascribed to a shortening of the spin-spin nuclear relaxation time T_2 (which follows a correspondent shortening of the spin-lattice relaxation time T_1) whereby the shortening of T_2 produces a decay of the transverse nuclear magnetization in a time shorter than the detection time of the spectrometer. The wipe-out results from a combination of a strong hyperfine coupling of nuclei to the electron spin and a slowing down of the fluctuations of the magnetic moment of the ions. Thus the wipe-out effects contains useful information about both the hyperfine coupling and the electron spin dynamics. The effect is a rather general phenomenon in NMR and has been observed previously in other systems such as spin glasses,[20] stripe-ordered cuprates,[21] and colossal magnetic resistance manganites.[22] In
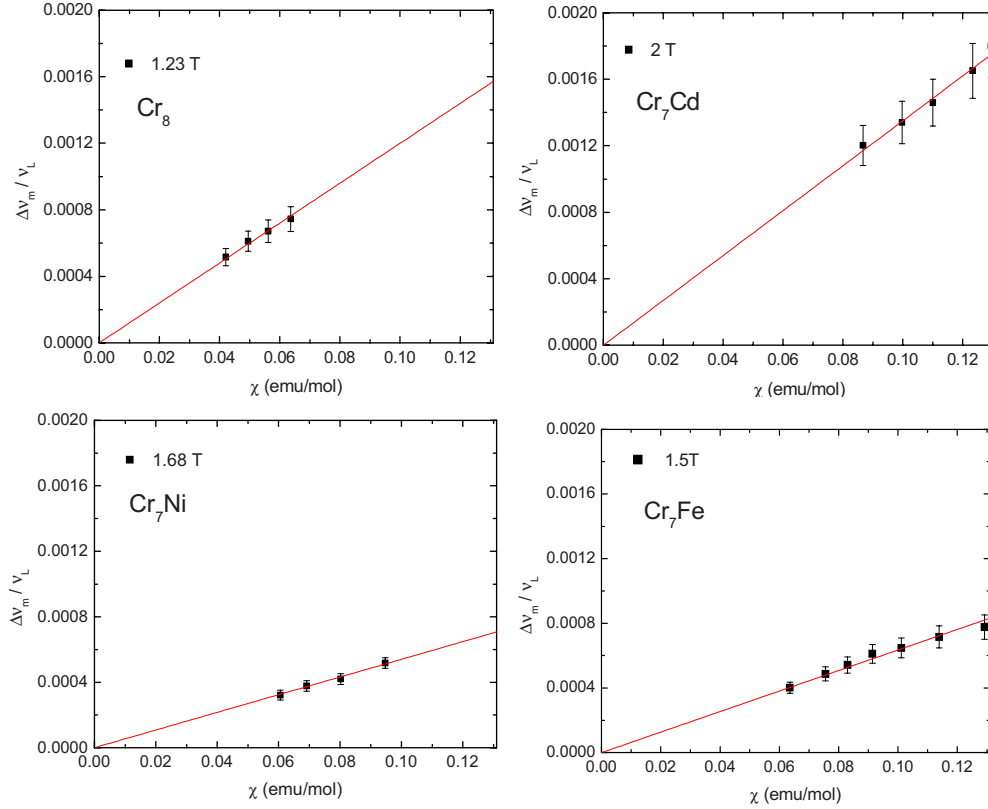
FIG. 5. (Color online) Inhomogeneous part of the linewidth, extracted as explained in the text, plotted vs magnetic susceptibility with temperature as implicit parameter.

particular, a loss of ^{1}H NMR signal on lowering the temperature has been observed previously in other molecular nanomagnets with a magnetic ground state.[9,23]

A quantitative analysis of the wipe-out effect was done successfully in Mn_6, Fe_4, and Fe_{19} molecular clusters[23] by using a simple and intuitive model which captures the main physical characteristics of the problem. The model allows for a semiquantitative determination of the relevant fluctuation frequency of the electron spin moment. In the following we present a summary of the wipe-out effect in the different heterometallic rings from which one can deduce a relative comparison of the spin dynamics in the different systems. The data of Cr_7Fe (Ref. 13) and partly Cr_7Ni (Ref. 14) have been published before while the data in Cr_8 and Cr_7Cd are new. We are going to analyze the wipe-out effect in our cases (Cr_7Fe, Cr_8, Cr_7Cd, and Cr_7Ni) by using the same model used before[23] which we summarize briefly in the following.

TABLE II. The average square dipolar coupling constant in Eq. (3) determined from the fits in Fig. 5 for the different rings.

Molecule	A'_z (Hz mol/G emu)^2	A_z (cm^{-6})
Cr_8	2600	5×10^{43}
Cr_7Cd	3250	6.4×10^{43}
Cr_7Ni	530	0.9×10^{43}
Cr_7Fe	730	0.9×10^{43}

We assume that the dominant contribution to T_2^{-1} is coming from the dephasing due to the hyperfine interactions with the exchange coupled magnetic ions. In the weak collision, fast motion approximation, the relaxation rate can be expressed in terms of the spectral density of the fluctuating hyperfine field at zero frequency as[18,24]

$$T_2^{-1} = \gamma_N^2 \langle \delta H_z^2 \rangle \tau(T) \propto \gamma_N^2 \frac{\langle \delta \mu_e^2 \rangle}{r^6} \tau(T), \qquad (4)$$

where δH_z is the local longitudinal fluctuating field originating from a magnetic moment at a distance r from the proton spin, and τ gives the correlation time, which is solely determined by the dynamics of the exchange coupled magnetic ions and can thus be temperature dependent. The central idea is that, on lowering the temperature, the correlation time $\tau(T)$ becomes progressively longer and thus the relaxation time T_2 becomes shorter [see Eq. (4)] until eventually it reaches the limiting value $\tau_d = 10^{-5}$ s which we estimate to be the limit of detectability of the NMR signal in our experimental setup. Since the dipolar hyperfine field and thus T_2 depends upon the distance r from the magnetic ions, the limiting value τ_d is reached progressively by all protons, with the ones closer being wiped-out first. To describe the wipe out we assume one central ion surrounded by a large number of protons homogeneously distributed at distances up to a maximum value R^*, the number density being $\rho = n_0/[(4\pi/3)(R^*)^3]$, where n_0 is the total number of protons in each molecule. Being in the regime of the wipe-out effect,
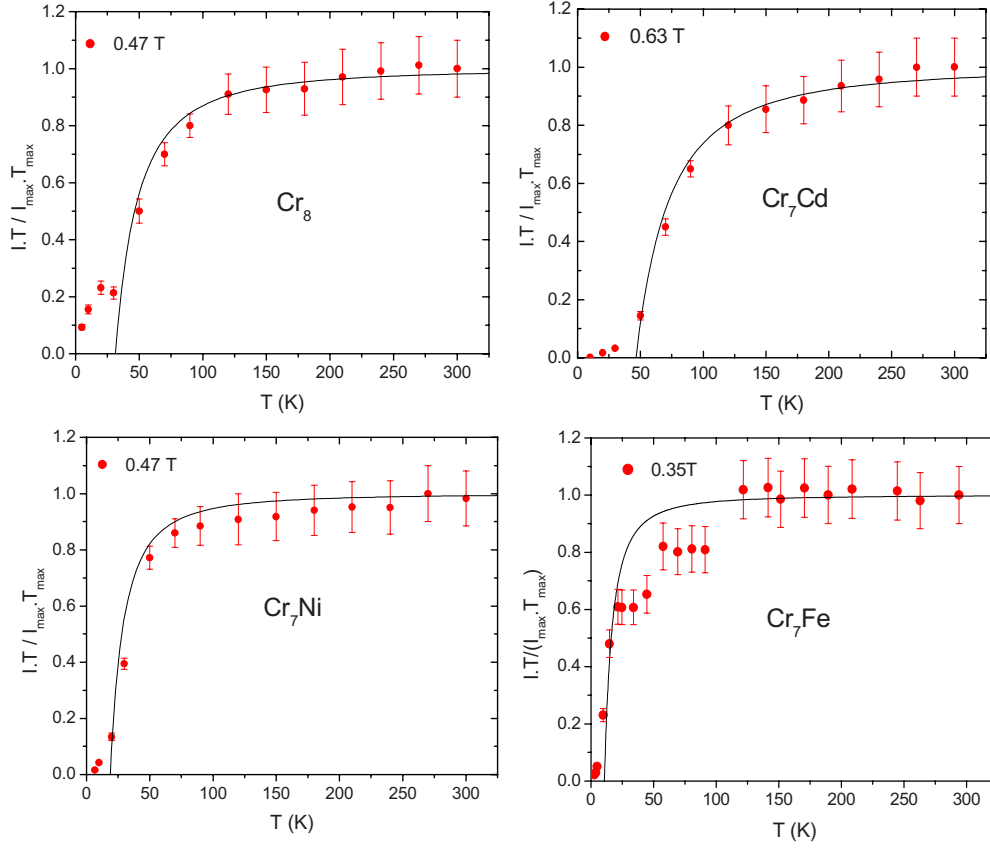
FIG. 6. (Color online) Signal intensity times the temperature normalized to the room-temperature value plotted vs temperature for the four rings. Without signal loss the plot should be temperature independent. The full lines are fits of the wipe-out effect using Eq. (6) with the fitting parameters given in Table II.

and for a given temperature or value of the correlation time $\tau(T)$, there is a number of protons having a T_2^{-1} value larger than the critical value of 10^5 s^{-1}. These protons are enclosed within a notional sphere of radius $r_c(T)$ and do not contribute to the measured signal intensity. On the other hand, the protons located outside this sphere can be detected and their number $n(T)$ can be written as

$$n(T) = n_0 \left[1 - \left(\frac{r_c}{R^*} \right)^3 \right]. \tag{5}$$

The value of the critical radius r_c in Eq. (5) can be obtained from Eq. (4) by setting $T_2^{-1} = \tau_d^{-1}$. Then one can express $n(T)$ in terms of the temperature-dependent correlation time $\tau(T)$ as

$$\frac{n(T)}{n_0} = 1 - \frac{\gamma_N \sqrt{\langle \delta\mu_e^2 \rangle} \sqrt{\tau_d}}{(R^*)^3} \sqrt{\tau(T)}. \tag{6}$$

In order to use Eq. (6) to fit the data, one has to make some educated guess about the functional form of the temperature dependence of the correlation time $\tau(T)$.

Previous NMR studies in a series of AFM rings have shown that the temperature dependence of the correlation time (extracted from the spin-lattice relaxation data) has the form of a power law $\tau(T) = cT^{-3.5}$ for all the rings.[25] Therefore we adopt the same expression to fit the wipe-out data also for our samples in Fig. 6, using Eq. (6). The two fitting

parameters for different rings, i.e., c and $\sqrt{\langle \delta\mu_e^2 \rangle}(R^*)^{-3}$, are given in Table III and the results of the fits are shown in Fig. 6 for the low-field data in which the wipe-out effect is more pronounced.

The theoretical curve reproduces well the sudden drop in intensity occurring at low temperature although a good fit over the whole temperature range is impossible due to the crudeness of the model. This is particularly evident in Cr$_7$Fe where the big drop in signal intensity occurs at lower temperature leaving an intermediate temperature range where the fit is poor. Thus the values of the fitting parameters in Table III have to be considered only indicative. The values of the coupling parameter $\sqrt{\langle \delta\mu_e^2 \rangle}(R^*)^{-3}$ are of the same order in all rings and are mainly due to the dipolar coupling of the protons with the magnetic moment of the ions. On the other

TABLE III. The two fitting parameters, i.e., c and $\sqrt{\langle \delta\mu_e^2 \rangle}(R^*)^{-3}$, for different rings according to Eq. (6).

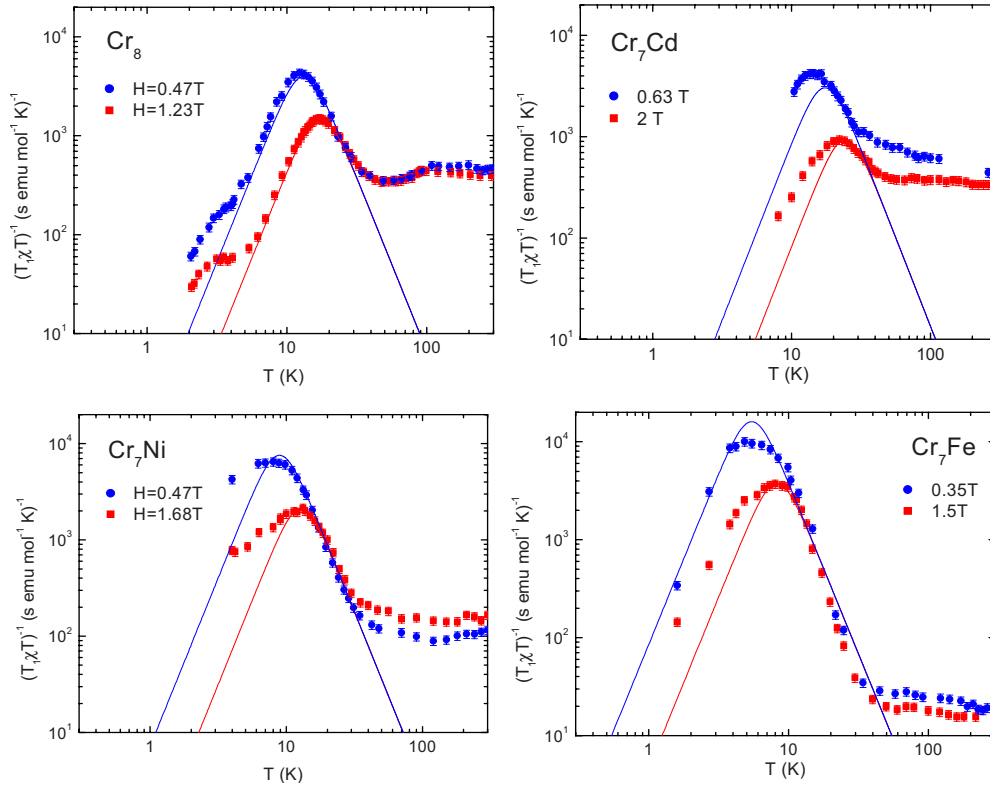| Molecule	c (s/rad)	$\sqrt{\langle \delta\mu_e^2 \rangle}(R^*)^{-3}$ (G)
Cr$_8$	0.66×10^{-4}	600
Cr$_7$Cd	1.33×10^{-4}	850
Cr$_7$Ni	1.6×10^{-5}	500
Cr$_7$Fe	4×10^{-6}	300

FIG. 7. (Color online) Proton spin-lattice relaxation rate divided by χT vs temperature for different rings at two values of the external field. The curves are fitted using Eq. (7) with two fitting parameters: A obtained from the high-field data, and ω_c obtained from the fit of the wipe-out effect in Fig. 6. The fitting parameters are given in Table IV.

hand the constant c which determines the correlation time $\tau(T) = cT^{-3.5}$ is more than one order of magnitude shorter in the Fe (and Ni) substituted ring with respect to the homometallic ring Cr_8. This effect of magnetic ion substitution on the spin dynamics in the ring will be confirmed in next section where it is shown that with the same correlation frequency, used to explain the wipe-out effect, we can fit the low-temperature peak in the spin-lattice relaxation rate T_1^{-1}.

C. Spin-lattice relaxation at low temperature

The temperature dependence of the proton spin-lattice relaxation rate is characterized by a strong peak centered at around 10–20 K and dependent on the external magnetic field as shown in Fig. 7 for the four rings at two values of the external magnetic field. This peak is typical of all molecular magnetic homometallic rings and clusters.[9,15] A qualitative explanation can be given which is related to the wipe-out effect. The slowing down of the fluctuation frequency $\omega_c = \tau^{-1} = c^{-1} T^{3.5}$, which is responsible for the shortening of T_2 as discussed in the previous paragraph, is also responsible for the shortening of T_1. However, while T_2 keeps shortening until ω_c becomes on the order of the static nucleus-electron coupling energy which, in frequency units, is in the kilohertz range, T_1^{-1} reaches a maximum when the correlation frequency ω_c becomes on the order of the nuclear Larmor frequency (in the megahertz range).[18] A rigorous theoretical approach has shown that at low temperature the fluctuations of the hyperfine field at the nuclear site are due to the relaxation

of the macroscopic magnetization of the ring, not to the fluctuations of the individual spin at the ion sites. This relaxation is dominated by a single correlation frequency which we identify with ω_c and is due to spin-phonon interactions.[16] A subsequent theoretical analysis has provided an explanation for the origin of the universal behavior of the slowing down of the magnetization fluctuations which is responsible for the observed peak.[25] In this experimental paper we analyze the data in a phenomenological way using a single correlation frequency to describe the electronic spin dynamics in the same way as done in Ref. 15. This will allow us to capture the relevant changes occurring in the spin dynamics when comparing the results in the heterometallic rings with the homometallic one Cr_8.

The simple expression for the relaxation rate can be obtained from the original Moriya theory of nuclear relaxation in paramagnets[18,24] under some simplifying assumptions, the main one being that the hyperfine field at the nuclear site is modulated by a dominant single correlation frequency which drives the relaxation and fluctuation of the ring magnetization.[14,16,25] The expression is

$$\frac{1}{T_1} = A' \chi T \frac{\omega_c(T)}{\omega_c^2(T) + \omega_L^2}, \qquad (7)$$

where $A' \chi T$ is the average square of the transverse fluctuating hyperfine field in frequency units, ω_L is the proton Larmor frequency, $\omega_c(T) = 1/\tau(T)$ is the characteristic frequency, and χ is the uniform magnetic susceptibility ex-

TABLE IV. Correlation frequency ω_c, the average square of the nuclear electron hyperfine fluctuation A', and the hyperfine field A for different molecular rings.

Molecule	ω_c (rad/s)	A' (rad^2 mol/s^2 emu K)	A (cm^{-6})
Cr$_8$	$1.5 \times 10^4 T^{3.5}$	1×10^{12}	4.5×10^{43}
Cr$_7$Cd	$0.75 \times 10^4 T^{3.5}$	1×10^{12}	4.5×10^{43}
Cr$_7$Ni	$6 \times 10^4 T^{3.5}$	1.9×10^{12}	9×10^{43}
Cr$_7$Fe	$2.5 \times 10^5 T^{3.5}$	3×10^{12}	14.4×10^{43}

pressed in electromagnetic unit/mole. The temperature dependence of χT (see Fig. 2) represents the amplitude of the local effective moments. Thus in order to isolate the dynamics from the static effects, we have plotted $(T_1 \chi T)^{-1}$ versus temperature as shown in Fig. 7. The data can now be fitted with two fitting parameters: A' related to the average square of the nuclear electron hyperfine fluctuations and $\omega_c(T)$ which can be assumed to be of the form $\omega_c(T) = \tau(T)^{-1} = c^{-1} T^{3.5}$ to be consistent with the wipe-out analysis of the previous paragraph and the results in other AFM rings.[15] The fitting parameters are given in Table IV.

As one can see in Fig. 7, the theoretical curves given by Eq. (7) reproduce qualitatively the relaxation data by using only one single fitting parameter, namely, A' while for the correlation frequency we used the values obtained from the analysis of the wipe-out effect. One should note that a good fit for temperatures less than 10 K is impossible anyway since the data at low temperature are affected by the wipe-out effect and thus they do not represent an average relaxation rate over all protons of the molecule.

From the value of A', one can obtain the square hyperfine interaction A in units of inverse volume using the following equation:

$$A = \frac{A'}{4 \pi (\hbar \gamma_n \gamma_e)^2}.$$

γ_n and γ_e are the gyromagnetic ratios for the nuclear and the electron, respectively.

The obtained values of the A for different molecular rings are also given in Table IV. The hyperfine field A corresponds essentially to the $(1/r^3)^2$ term in the nuclear-electron dipolar interaction. The obtained values are all of the same order of magnitude reflecting the fact that the average distance between protons and magnetic ions is very similar in all rings. Furthermore the values of the hyperfine coupling constant obtained from relaxation data (Table IV) are of the same order of magnitude as the ones obtained from linewidth data (Table II) indicating that in both cases the dominant interaction is the nuclear-ion dipolar interaction.

On the other hand, the correlation frequency ω_c is much higher in the Ni and Fe substituted rings. This can be seen well in Fig. 8 where we show the correlation frequency extracted from Eq. (7) with the experimental data for the nuclear-spin-lattice relaxation and by using the values of A' in Table IV. The results are shown in Fig. 8 together with the
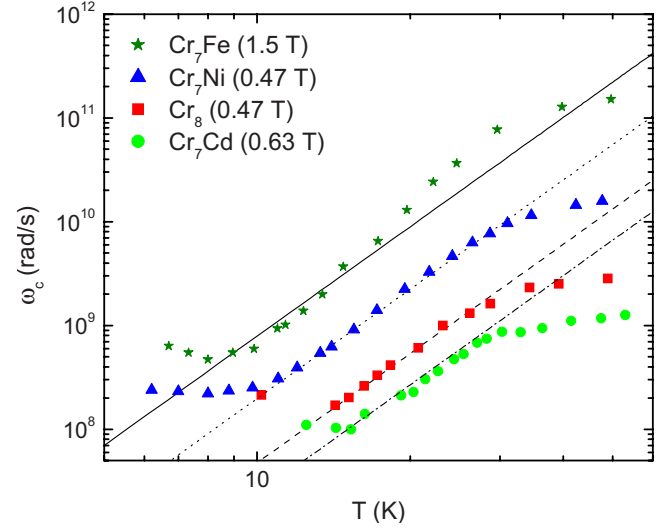

FIG. 8. (Color online) Correlation frequencies for different molecular magnets extracted from the NMR experimental data plotted vs temperature. The solid, dot, dashed, and dashed-dotted lines correspond to the behavior of $\omega_c(T)$ for Cr$_7$Fe, Cr$_7$Ni, Cr$_8$, and Cr$_7$Cd, respectively, which are obtained from the relaxation and wipe-out effect (see Table IV).

lines representing the best fit for the T dependence of ω_c given in Table IV.

The dramatic effect of the ion substitution in the ring on the relaxation spin dynamics at low temperature is a central finding of this paper. Since the relaxation of the ring magnetization at low temperature is believed to be due to spin phonon interaction[16,25] the much higher correlation frequency in the Ni and Fe substituted rings must be associated to much stronger crystal-field effects in the latter heterometallic rings. It should be remarked, however, that two assumptions made here, based on previous work in homometallic AFM rings, could be subject to criticism. One regards the assumption of a single correlation function (CF) since it was found that in heterometallic rings, particularly in the temperature region of the peak in T_1^{-1}, the spin-spin correlation function shows a multi-Lorentzian regime.[14,26] The second assumption is the one leading to the proportionality of T_1^{-1} to χT [see Eq. (7)]. Both effects are the consequence of a nonuniform distribution of the local magnetic moments in the heterometallic rings. These effects should be taken into consideration in a detailed theoretical explanation of the present data, which is outside the scope of the present paper.

D. Spin-lattice relaxation at high temperature

As can be seen in Fig. 7 the temperature dependence of the proton spin-lattice relaxation rate changes for all the rings at temperatures above about 30–40 K. Above this temperature and up to room temperature, $(T_1 \chi T)^{-1}$ is weakly temperature and field dependent and it departs completely from the behavior predicted by Eq. (7) with the fitting parameters in Table IV. The changeover of behavior of the nuclear relaxation rate is most likely related to the changeover from a correlated spin dynamics at low temperature,
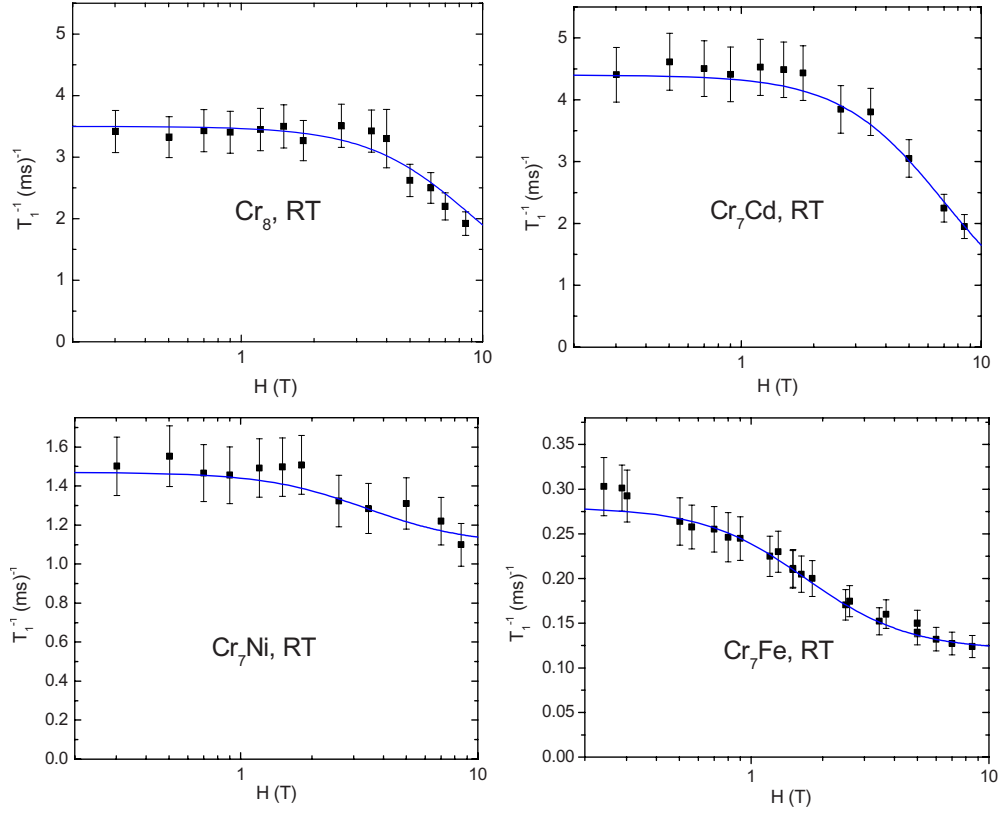
FIG. 9. (Color online) Proton spin-lattice relaxation rate vs external magnetic field at RT for the four investigated rings. Note, in comparing, that for Cr_7Ni and Cr_7Fe the vertical scale is magnified. The full lines are fitting curves as explained in the text.

whereby the local spin dynamics is driven by the relaxation of the macroscopic magnetization to a high-temperature spin dynamics. For the $k_B T > J$ the local spins of the magnetic ions fluctuate almost independently from each other. Another important effect to be noted is that above 40 K the magnitude of $(T_1 \chi T)^{-1}$ is much smaller for the Ni and Fe heterometallic rings with respect to the homometallic ring Cr_8 as well as the diamagnetically substituted ring Cr_7Cd (see Fig. 7). To explore more quantitatively this effect, we have performed a series of measurements of T_1^{-1} as a function of external magnetic field at room temperature (RT) for four rings. The results are shown if Fig. 9 for all the rings.

To explain the high-temperature data we refer to the original Moriya theory of nuclear relaxation in paramagnetic materials.[24] In the weak collision approximation one can write

$$T_1^{-1} \alpha \sum_{ij} \alpha_{ij} J_{\pm}^{ij}(\omega_e) + \sum_{ij} \beta_{ij} J_z^{ij}(\omega_N), \quad (9)$$

where i and j number the electronic spins, ω_e and ω_N are the Larmor frequencies of the electron and of the nucleus, respectively, α_{ij} and β_{ij} are geometrical factors of the nuclear-electron dipolar interaction, and $J_{\pm}^{ij}$ and J_z^{ij} are the transverse and longitudinal spectral densities of the spin fluctuations, respectively. In Eq. (9), the spectral density $J_{\pm,z}^{ij}(\omega)$ can be expressed by the FT of the spin CF,

$$J_{\pm,z}^{ij}(\omega) = \int G_{\alpha}^{ij}(r,t) e^{i\omega t} dt, \quad (10)$$

where $\alpha = \pm, z$ corresponds to the transverse and longitudinal components, respectively.

For uncorrelated spins, namely, $T \gg J/k_B$, one can assume that the CF decays as a Gaussian or an exponential[24] with a correlation frequency which is due to the rapid exchange of energy between adjacent electronic spins with an exchange frequency given approximately by[24]

$$\Gamma_{exc} = (2\pi J/h)[S(S+1)]^{1/2}. \quad (11)$$

Thus in the simplest approximation one can write for the relaxation rate

$$T_1^{-1} = K \left\{ \frac{1}{2} A^{\pm} [\Gamma_{exc}/(\omega_e^2 + \Gamma_{exc}^2) + A^z \Gamma_{exc}/(\omega_N^2 + \Gamma_{exc}^2)] \right\}$$

$$\cong K \left\{ \frac{1}{2} A^{\pm} [\Gamma_{exc}/(\omega_e^2 + \Gamma_{exc}^2) + A^z/\Gamma_{exc}] \right\}, \quad (12)$$

where we assumed $\omega_N \ll \Gamma_{exc}$ and the constants $A^{\pm}$ and A^z are averages over all protons in the molecule of the products of the hyperfine dipolar tensor components α_{ij} and β_{ij}, respectively [see Eq. (9)]. The constant K, which has been factored out from the dipolar tensor coefficients, is given by $K = (h\gamma_N\gamma_e)^2/4\pi = 1.94 \times 10^{-32} (s^{-2} cm^6)$ where the electronic and nuclear gyromagnetic ratios are defined by the Larmor relation $\omega_e = \gamma_e H$ and $\omega_N = \gamma_N H$, respectively. For both Cr_8 and Cr_7Cd, Eq. (12) should hold and the data in Fig. 9 can be fitted (solid lines) with the following choice of parameters: $\Gamma_{exc} = 1.6 \times 10^{12}$ (rad Hz); $A^{\pm} = 4.7 \times 10^{47}$ cm^{-6}; and $A^z = 4.9$

$\times 10^{46}$ cm^{-6} for the Cr$_8$, and $\Gamma_{exc} = 1.2 \times 10^{12}$(rad Hz); $A^{\pm} = 5.2 \times 10^{47}$ cm^{-6}; $A^z = 1.9 \times 10^{46}$ cm^{-6} for the Cr$_7$Cd.

The value of the exchange frequency is indeed of the order predicted by Eq. (11) for the appropriate J coupling of the ring and the dipolar coupling coefficients are consistent with the proton-ion distance in the ring. It should be noted that for an isotropic Heisenberg exchange system of identical electronic spins, the CF of the transverse spin components $S_{\pm}(t)$ contains a term randomly varying multiplied by a coherent electronic Larmor precession around the external magnetic field.[24] Thus the CF in Eq. (10) contains a term $G_{\pm}$ proportional to $\langle S'_{\pm}(t) S'_{\pm}(0) \rangle e^{-i\omega_e t}$. When one takes the FT, according to the Eq. (10), one obtains a spectral density $J_{\pm}(\omega)$ centered at $\omega_e \pm \omega_N \cong \omega_e$, as it appears in the first term of Eq. (9). If the spin system is no longer isotropic and/or is made up of nonequivalent moments, i.e., there is a symmetry breaking in the plane perpendicular to the magnetic field as in the case of the heterometallic rings, one expects that the coherent electronic Larmor precession is damped. Consequently, the term of Eq. (10) containing the transverse CF, should probe the spectral density at ω_N, as for the longitudinal fluctuations. This observation is of paramount importance to explain the difference in magnitude of T_1^{-1} for the different rings (see Figs. 7 and 9).

In the two rings with magnetic substitution, i.e., Cr$_7$Ni and Cr$_7$Fe, one expects a breakdown of the assumption of isotropic Heisenberg exchange between equivalent magnetic moments and thus Eq. (12) should be replaced by

$$T_1^{-1} = K \left\{ \frac{1}{2} A^{\pm} [\Gamma_{exc}^{\pm} / (\omega_N^2 + \Gamma_{exc}^{\pm 2}) + A^z / \Gamma_{exc}^z] \right\}$$
$$= K \left[\frac{1}{2} A^{\pm} (1/\Gamma_{exc}^{\pm}) + A^z / \Gamma_{exc}^z \right], \quad (13)$$

where we assumed $\omega_N \ll \Gamma_{exc}$ and the exchange frequencies may be different from the isotropic case and different for transverse ($\Gamma_{exc}^{\pm}$) and longitudinal (Γ_{exc}^z) fluctuations.

The contributions described by Eqs. (12) and (13) refer to homometallic and heterometallic rings, respectively. Theses two equations lead, in agreement with the results in Fig. 7, to a temperature-independent behavior of $(T_1 \chi T)^{-1}$, since the exchange frequency is T independent. The field dependence observed in the data in Fig. 9 for Cr$_8$ and Cr$_7$Cd arise from the term $\omega_e = \gamma_e H$ present in Eq. (12). On the other hand Eq. (13), valid for the heterometallic rings Cr$_7$Ni and Cr$_7$Fe, predict no field dependence while it is clear that the field dependence is present also in the heterometallic rings (see Fig. 9). In order to explain the field dependence in Cr$_7$Ni and Cr$_7$Fe, one should thus postulate an additional contribution to the proton relaxation arising from the interaction of the protons with the heterometallic ion. This additional contribution can be put in the form,

$$T_1^{-1} = K A_h^z \frac{\Gamma_T}{\omega_N^2 + \Gamma_T^2}, \quad (14)$$

which is the expression of the nuclear relaxation due to a paramagnetic "impurity" with correlation frequency Γ_T. The dipolar coupling constant A_h^z is expected to be smaller than

the constants $A^{\pm}$ and A_z in Eq. (12) because on the average the protons are further away from the Fe^{2+} (Ni^{2+}) moments. Thus the data in Fig. 9 for Cr$_7$Ni and Cr$_7$Fe can be tentatively fitted by an expression of the form,

$$T_1^{-1} = K \left[\frac{1}{2} A^{\pm} (1/\Gamma_{exc}^{\pm}) + A^z / \Gamma_{exc}^z \right] + K A_h^z \frac{\Gamma_T}{\omega_N^2 + \Gamma_T^2}. \quad (15)$$

The full curves in Fig. 9 for Cr$_7$Ni and Cr$_7$Fe correspond to Eq. (15) with the following fitting parameters: $K[A^{\pm}/2\Gamma_{exc}^{\pm} + A^z/\Gamma_{exc}^z] = 1100$ s^{-1}; $A_h^z = 1.7 \times 10^{43}$ cm^{-6}; and $\Gamma_T = 9 \times 10^8$ rad Hz for Cr$_7$Ni, and $K[A^{\pm}/2\Gamma_{exc}^{\pm} + A^z/\Gamma_{exc}^z] = 120$ s^{-1}; $A_h^z = 3.8 \times 10^{42}$ cm^{-6}; and $\Gamma_T = 4.6 \times 10^8$ rad Hz for Cr$_7$Fe.

Regarding the first term in Eq. (15), one can observe that it corresponds to what expected on the basis of the same coupling constants $A^{\pm}$ and A^z, derived above for Cr$_8$ and Cr$_7$Cd, and exchange frequencies, $\Gamma_{exc}^{\pm}$ and Γ_{exc}^z, almost one order of magnitude larger for Cr$_7$Fe. This is not surprising since in the heterometallic rings the damping process of the precession of the spin due to inequivalency of the adjacent moments and/or the anisotropy can speed up the decay of the electronic correlation function. On the other hand, the energy conserving exchange fluctuations are not allowed for the Fe^{2+} (Ni^{2+}) moments since they are different from the nearest-neighbor Cr^{3+} moments. Thus only longitudinal spin-lattice fluctuations are allowed for the substituted ion. The value of the correlation frequency Γ_T for the longitudinal fluctuations of the Fe^{2+} (Ni^{2+}) moment, is consistent with a slow fluctuation of the impurity spin due to the spin-lattice relaxation. The consistency of the small coupling constants A_h^z is more difficult to be determined in view of the semi-quantitative model adopted.

V. SUMMARY AND CONCLUSIONS

We have presented and compared susceptibility and NMR data in three heterometallic rings with the corresponding homometallic ring Cr$_8$. The singlet ground state, $S=0$, of the antiferromagnetic coupled ring Cr$_8$ is modified into a magnetic ground state with total spin $S=3/2$ for Cr$_7$Cd, $S=1/2$ for Cr$_7$Ni and Cr$_7$Fe. The nearest-neighbor magnetic exchange coupling remains antiferromagnetic in all rings with a small change in the value of the effective J. Regarding the spin dynamics we have found that the proton relaxation rate is driven by a mechanism different at low temperature from the one at high temperature. For $T < J/k_B$ the magnetic moments of the ions are strongly correlated and the nuclear relaxation is due to the modulation of the hyperfine field by the relaxation process of the total magnetization of the ring.[15,16,25] The relaxation process of the magnetization is dominated in AFM rings by a single correlation frequency ω_c which is driven by spin-phonon interaction and is thus strongly temperature dependent.[14,16,25] This single correlation frequency can be extracted from nuclear relaxation measurements via a simple model.[15] By using here this simple model we were able to compare the spin dynamics in homometallic and heterometallic rings whereby we found a much higher correlation frequency for Cr$_7$Ni and even higher for Cr$_7$Fe.

This is a clear evidence of enhanced spin-phonon interaction in the heterometallic rings due most likely to the strong single ion anisotropy of, e.g., Fe^{2+} as also found in Mossbauer measurements.[27] For $T > J/k_B$ the magnetic moments of the ions become weakly correlated and the proton relaxation is dominated by the fluctuations of the individual paramagnetic moments. In this high-temperature region we have observed a drastic difference in the values of the T_1^{-1} in Cr_8 and Cr_7Cd when compared to Cr_7Ni and Cr_7Fe. We have interpreted the effect as due to the change in the electron spin correlation function, whereby in the homometallic Cr_8 and weakly perturbed Cr_7Cd rings the coherent precession of the spin around the applied field predicted for the transverse components in the isotropic Heisenberg model is allowed, while in the strongly perturbed Cr_7Ni and more so in Cr_7Fe this precession is completely overdamped. This agrees with the notion that in Cr_7Ni and Cr_7Fe the spin dynamics is perturbed by the substituted magnetic ion and that the distribution of spin density in the ring is nonuniform. The local spin-density redistribution in the ring could be obtained, in principle, from NMR measurements. As a matter of fact the local distribution of the spin density at the different ion sites in the ground state was measured in a previous publication in Cr_7Cd by ^{57}Cr NMR and found to remain rather uniform over the ring.[6] We have attempted to measure the spin density in the other heterometallic rings but the NMR signal of ^{53}Cr, ^{57}Fe, and ^{61}Ni could not be detected down to 1.4 K due to the combination of poor signal to noise ratio and very short T_2. A recent Mossbauer investigation of Cr_7Fe has shown a reduction in the expectation value of the Fe^{2+} ($s = 2$) spin moment to $\langle s \rangle = 0.9$ and a strong magnetic single-ion anisotropy.[27] Thus measurements of NMR at the ^{53}Cr site appear to be essential and will be attempted again at very low temperature by the use of a dilution refrigerator. Indirect evidence of a strong perturbation of the Cr spin density by insertion of Fe and Ni ions is inferred indirectly from the spin dynamics as discussed above.

*Corresponding author; houshang.amiri@unipv.it

[1] O. Kahn, *Molecular Magnetism* (VCH, Berlin, 1990); D. Gatteschi, R. Sessoli, and J. Villain, *Molecular Nanomagnets* (Oxford University Press, New York, 2006).

[2] I. S. Tupitsyn and B. Barbara, in *Magnetism: Molecules to Materials III*, edited by J. Miller and M. Drillon (Wiley-VCH, Weinheim, Germany, 2002).

[3] E. del Barco, A. D. Kent, S. Hill, J. M. North, N. S. Dalal, E. M. Rumberger, D. N. Hendrickson, N. Chakov, and G. Christou, J. Low Temp. Phys. **140**, 119 (2005); W. Wernsdorfer, Adv. Chem. Phys. **99**, 118 (2001).

[4] M. Affronte, T. Guidi, R. Caciuffo, S. Carretta, G. Amoretti, J. Hinderer, I. Sheikin, A. G. M. Jansen, A. A. Smith, R. E. P. Winpenny, J. van Slageren, and D. Gatteschi, Phys. Rev. B **68**, 104403 (2003).

[5] F. K. Larsen, E. J. L. McInnes, H. ElMkami, J. Overgaard, S. Piligkos, G. Rajaraman, E. Rentschler, A. A. Smith, G. M. Smith, V. Boote, M. Jennings, G. A. Timco, and R. E. P. Winpenny, Angew. Chem., Int. Ed. **42**, 101 (2003).

[6] E. Micotti, Y. Furukawa, K. Kumagai, S. Carretta, A. Lascialfari, F. Borsa, G. A. Timco, and R. E. P. Winpenny, Phys. Rev. Lett. **97**, 267204 (2006).

[7] F. Troiani, M. Affronte, S. Carretta, P. Santini, and G. Amoretti, Phys. Rev. Lett. **94**, 190501 (2005); F. Troiani, A. Ghirri, M. Affronte, S. Carretta, P. Santini, G. Amoretti, S. Piligkos, G. Timco, and R. E. P. Winpenny, *ibid.* **94**, 207208 (2005).

[8] G. A. Timco, S. Carretta, F. Troiani, F. Tuna, R. J. Pritchard, E. J. L. McInnes, A. Ghirri, A. Candini, P. Santini, G. Amoretti, M. Affronte, and R. E. P. Winpenny, Nat. Nanotechnol. **4**, 173 (2009).

[9] F. Borsa, A. Lascialfari, and Y. Furukawa, in *Novel NMR and EPR Techniques*, edited by J. Dolinsek, M. Vilfan, and S. Zumer (Springer, New York, 2006).

[10] N. V. Gerbeleu, Yu. T. Struchkov, G. A. Timco, A. S. Batsanov, K. M. Indrichan, and G. A. Popovich, Dokl. Akad. Nauk SSSR **313**, 1459 (1990).

[11] J. van Slageren, R. Sessoli, D. Gatteschi, A. A. Smith, M. Helliwell, R. E. P. Winpenny, A. Cornia, A.-L. Barra, A. G. M. Jansen, E. Rentschler, and G. A. Timco, Chem.-Eur. J. **8**, 277 (2002).

[12] M. Affronte, A. Ghirri, S. Carretta, G. Amoretti, S. Piligkos, G. A. Timco, and R. E. P. Winpenny, Appl. Phys. Lett. **84**, 3468 (2004).

[13] H. Amiri, M. Mariani, A. Lascialfari, F. Borsa, G. A. Timco, F. Tuna, and R. E. P. Winpenny, Phys. Rev. B **81**, 104408 (2010).

[14] A. Bianchi, S. Carretta, P. Santini, G. Amoretti, Y. Furukawa, K. Kiuchi, Y. Ajiro, Y. Narumi, K. Kindo, J. Lago, E. Micotti, P. Arosio, A. Lascialfari, F. Borsa, G. Timco, and R. E. P. Winpenny, J. Magn. Magn. Mater. **322**, 1262 (2010); A. Bianchi *et al.* (unpublished).

[15] S. H. Baek, M. Luban, A. Lascialfari, E. Micotti, Y. Furukawa, F. Borsa, J. van Slageren, and A. Cornia, Phys. Rev. B **70**, 134434 (2004).

[16] P. Santini, S. Carretta, E. Liviotti, G. Amoretti, P. Carretta, M. Filibian, A. Lascialfari, and E. Micotti, Phys. Rev. Lett. **94**, 077203 (2005).

[17] M. Affronte *et al.*, Polyhedron **24**, 2562 (2005).

[18] C. P. Slichter, *Principles of Magnetic Resonance* (Springer-Verlag, New York, 1996).

[19] P. Khuntia, M. Mariani, M. C. Mozzati, L. Sorace, F. Orsini, A. Lascialfari, F. Borsa, C. Maxim, and M. Andruh, Phys. Rev. B **80**, 094413 (2009).

[20] D. A. Levitt and R. E. Walstedt, Phys. Rev. Lett. **38**, 178 (1977).

[21] A. W. Hunt, P. M. Singer, K. R. Thurber, and T. Imai, Phys. Rev. Lett. **82**, 4300 (1999).

[22] G. Papavassiliou, M. Belesi, M. Fardis, and C. Dimitropoulos, Phys. Rev. Lett. **87**, 177204 (2001).

[23] M. Belesi, A. Lascialfari, D. Procissi, Z. H. Jang, and F. Borsa, Phys. Rev. B **72**, 014440 (2005).

[24] T. Moriya, Prog. Theor. Phys. **16**, 23 (1956); **28**, 371 (1962).

[25] I. Rousochatzakis, A. Lauchli, F. Borsa, and M. Luban, Phys. Rev. B **79**, 064421 (2009).

[26] P. Santini *et al.* (unpublished).

[27] L. Cianchi, F. Del Giallo, M. Lantieri, P. Moretti, G. Spina, G. Timco, and R. Winpenny, Solid State Commun. **150**, 903 (2010).